Pramana – J. Phys. (2019) 93:55
https://doi.org/10.1007/s12043-019-1823-2

Structure, stability and electronic properties of bimetallic atomic chains of Au–Ag and Au–Pt

MUDRA R DAVE* and A C SHARMA

Physics Department, The Maharaja Sayajirao University of Baroda, Vadodara 390 002, India
*Corresponding author. E-mail: mudra.msu@gmail.com

MS received 27 December 2018; revised 3 April 2019; accepted 24 April 2019

Abstract. Quantum confinement of electrons in atomic chains provides the most powerful and versatile means to control electronic, optical, magnetic and thermoelectric properties of materials needed to make diodes, spin valves and optical labels. Furthermore, the alloying of metallic atoms in different compositions produces novel mechanical, electronic and chemical behaviours in bimetallic chains as well as in other structures. This motivated us to perform theoretical investigations on the structure, stability, magnetic and electronic properties of bimetallic atomic chains of Au–Ag and Au–Pt, by using Vienna *ab-initio* simulation package (VASP), which is based on the density functional theory (DFT) within generalised gradient approximation. We have used tension and cohesive energy criteria to assess the stability of the Au–Ag and Au–Pt atomic chains. A comparison between the computed cohesive energies of various possible structures are made to suggest the most probable chain structures that can occur in break junction experiments. Our computed results suggest that the ground state of the Au–Ag and Au–Pt atomic chains should have zig-zag geometry. Furthermore, the most favoured chain structures that can be formed at the last stage of nanowires stretching are: (i) an atomic chain with alternate arrangement of equal number of Au and Ag/Pt atoms and (ii) an atomic chain where two Ag/Pt atoms are separated by one Au atom. Our results on the electronic band structure and optical properties suggest that the Au–Ag atomic chain could be of semiconducting nature, while the most stable Au–Pt chain is metallic in nature. A spin-polarised calculation with the inclusion of spin–orbit coupling shows that the Au–Pt atomic chains are magnetic, if the number of Au atoms is not more than the number of Pt atoms.

Keywords. Bimetallic nanostructures; atomic chains; Au–Ag; Au–Pt.

PACS Nos 73.21.Hb; 71.20.Be; 73.63.Rt

1. Introduction

The dream of making devices with materials whose electrical, optical, magnetic and thermoelectric properties can be controlled by the use of quantum confinement, motivated researchers over the years to work on molecules, nanomaterials and atomic structures. Devices such as diodes, spin valves and optical labels can be made using quantum-confined electron systems. Compared to traditional electronic devices, devices made from molecules, nanomaterials and atomic structures have many unparalleled advantages like numerous degrees of freedom and an extremely reduced size. Properties of a material can be changed (a) by varying dimensionality and (b) by changing the relative concentration of different kinds of atoms in it. The alloying of metallic atoms produces novel mechanical, electronic and chemical behaviours. On changing the elemental composition and relative concentration of atoms, properties of an alloy can be changed over a wide range. For example, the optical absorption band in Ag–Au particles can be continuously shifted from the Ag to the Au position by increasing the Au mass ratio in the alloy [1]. Thus, the concentration and arrangement of different species in an alloy play an important role in changing its properties. The formation of an atomic chain can take place during nanowire stretching in mechanically controllable break junction (MCBJ) and high-resolution transmission electron microscopy (HRTEM) experiments [2–9]. There have been a large number of theoretical studies on the formation of stable metal atomic chains that can be formed during break junction experiments [10–19]. Theoretical approaches for synthesising the atomic chains are based on the minimisation of enthalpy,

Published online: 15 July 2019

cohesive energy and string tension [16–19]. It has been pointed out that the approach based on minimising the string tension is a better theoretical criterion to judge the stability of chains that can be formed during break junction experiments [16,17]. The prediction of chain formation based on tension criteria correlates well with the experimental observation in several cases [17,18].

There has been an intensive search for elements that can be used to form stable atomic chains [15,17,20,21]. Despite the initial reports that 3d and 4d row elements can be used to make atomic chains, unequivocal proof for the existence of stable atomic chains was found only for Au, Ag, Pt and Ir elements [17]. The strongest tendency for chain formation had been observed in Au and Pt atoms [17,22]. The most extensively and widely studied nanowires and linear atomic chains are those which are made of Au [6,11,14,16,23,24]. It is now well established that the tendency of chain formation is the strongest in Au atoms, compared to other metal atoms, and the Au-nanocontacts possess higher stability because of the low reactivity of Au atoms [17,22,25]. Although the formation of Ag-atomic chains has not been observed, stable chains of Au–Ag atoms have been realised experimentally [26]. The enhanced stability of Au–Ag alloy nanocontacts, compared to that of pure Au or Ag noncontacts, has been reported [13]. It has been found that the nanocontacts of the Au–Ag alloy are stable at larger atomic distances, which are breaking points for pure Au and Ag nanocontacts [13]. The experimental realisation of the Au–Ag bimetallic linear atomic chains [24] led to many theoretical investigations on the understanding of the mechanism and physical parameters (which are detrimental to chain formation), stability and the chemical composition of single atomic chains. Atomic chains were observed in experiments like the mechanical stretching of nanocontacts and break junction technique [13,18,19]. Such studies have established a correlation between the initial chemical composition of nanowires, atomic arrangement of single atomic chains in the final stage of stretching and direction of stretching [18,19]. There exist several experimental and theoretical studies on Au–Ag chains, and fewer studies were performed on Au–Pt chains [27,28]. Furthermore, the relative stability of the possible Au–Ag and Au–Pt chains has not been studied in the past. This motivated us to perform a study on relative stability to find the most probable bimetallic chains of Au–Ag and Au–Pt that can formed in MCBJ.

Past studies on bimetallic chains can broadly be divided into two categories: (i) chains which have an equal number of two types of atoms and (ii) chains which have an unequal number of two types of atoms, in a unit cell [18,19]. A majority of properties of atomic chains can be covered by these two types of chain structures. In view of this, we have chosen four possible structures: (a) type-A that has one Au and one Ag/Pt atom per unit cell, (b) type-B that has two Au and two Ag/Pt atoms per unit cell, (c) type-C that has two Au and one Ag/Pt atoms per unit cell and (d) type-D having one Au and two Ag/Pt atoms in a unit cell. Types A and B have an equal number of Au and Ag/Pt atoms in a unit cell, while types C and D consist of an unequal number of Au and Ag/Pt atoms in a unit cell.

The aim of our investigations is to find (i) possible stable chain structures and the most stable chain structures, (ii) structural parameters and (iii) electronic and magnetic properties of Au–Ag and Au–Pt bimetallic atomic chains that can be made with differing atomic arrangements. The four structures studied in this paper broadly represent two cases of uniformly and non-uniformly mixed bimetallic atoms. Such choice of atomic arrangements in the unit cell covers three major possible mixing in a bimetallic structure, which are evenly mixed, Au enhanced and Ag (or Pt) enhanced alloy chains. The paper is divided into four sections. Details of the computational methods used to perform our investigations are reported in §2. The obtained results are discussed in §3 and our results are summarised in §4.

2. Computational details

We have used a free-standing infinite chain model for computing our results. For computing chain structures, we have chosen a three-dimensional tetragonal unit cell having a chain along the z-axis and a large vacuum of 20 Å along the x- and y-directions, to separate the chain from periodic images and interaction. The accurate frozen-core full-potential projector augmented-wave (PAW) [29] method, based on the density functional theory implemented using the Vienna *ab-initio* simulation package (VASP) [30,31], is used to obtain the results reported in this paper. The generalised gradient approximation (GGA), for the exchange-correlation functional, has been applied to the Perdew–Burke–Ernzerhof (PBE) functional [32]. Brillouin zone sampling is done using a plane-wave basis set and the Monkhorst–Pack [33] scheme that uses $1 \times 1 \times 40$ in the full Brillouin zone with Gaussian smearing having a 0.01 smearing parameter. A 450 eV kinetic energy cut-off is used for computing the results which are sufficiently high to eliminate the discontinuity in convergence due to the finite points and different sizes of the unit cells [34]. This choice of the k-point mesh and cut-off energy provides us a total energy convergence within 1 meV.

The minimum energy configuration of each atomic chain was determined by simultaneously optimising the

unit cell size and ionic positions of atoms in the unit cell. The size of the unit cell was optimised by locating the minimum in the calculated cohesive energy per atom, as a function of $\bar{d}_z$, where $\bar{d}_z$ is the projection of the interatomic distance along the chain axis. The cell size is determined in terms of $\bar{d}$. For two atom unit cells, the size of the unit cell is $2 \times \bar{d}_z$, while for three and four atoms, the size of the unit cell is $3 \times \bar{d}_z$ and $4 \times \bar{d}_z$, respectively. For each value of $\bar{d}_z$, total energy was calculated for a range of x- and y-coordinates of each atom and a local minimum of total energy is determined. The global minimum is the minimum of the set of local minimums corresponding to a range of $\bar{d}_z$. After finding the optimum value of the $\bar{d}_z$ parameter, and ionic coordinates in the x- and y-directions, ionic relaxation was performed using the conjugate gradient minimisation scheme, until the minimum force acting on each atom was reduced to less than 1 meV/Å. Such minimisation ensures vibrationally stable structures.

3. Results and discussion

In this section, we discuss our results for four possible structures of Au–Ag and Au–Pt chains.

3.1 *Structure and stability*

The theoretical investigations performed in the past on atomic structures suggest that the criteria based on the string tension of a chain, instead of its total energy, are better in judging the stability and the corresponding geometrics of a structure. Tension being the first-order derivative of energy, the stable structure that corresponds to the minimum total energy can be realised where tension approaches zero from the infinitesimal initial negative value. Such criteria of tension to derive stable structures are very well reflected in the experimental observation of pristine Au, Ag and Pt atomic chains, as well as bimetallic atomic chains of Au–Ag [17,18]. Tension can be defined by $T = \mathrm{d}E/\mathrm{d}\bar{d}_z$,while cohesive energy E_{coh} of every structure can be computed using

$$E_{\mathrm{coh}} = \frac{1}{a+b}\left(E_{\mathrm{tot}} - aE_{\mathrm{atom}}^{\mathrm{Au}} - bE_{\mathrm{atom}}^{\mathrm{Pt\ or\ Ag}}\right), \qquad (1)$$

where E_{atom} is the energy of the Au, Ag and Pt atoms in free states, integers a and b are the number of atoms of Au and Ag (Pt) and E_{total} is the total energy of the bimetallic atomic chain. Our computed T and E_{coh} for types A, B, C and D atomic chains of Au–Ag and Au–Pt are displayed in figure 1 as the functions of $\bar{d}_z$.

As can be seen from figure 1, all the atomic chain structures of Au–Ag and Au–Pt exhibit a minimum in E_{coh} at the points where tension changes its sign. Our computed $\bar{d}_z$, from minimum energy structures, for types A, B, C and D chains of Au–Ag is equal to 2.31, 2.29, 2.49 and 2.50 Å, respectively. For the Au–Pt atomic chains, the minima energy structures of types A, B, C and D are observed when $\bar{d}_z = 2.25$, 2.23, 2.40 and 2.28 Å, respectively. The minimum energy structures deduced by string tension criteria are further relaxed using conjugate gradient algorithm. It is to be noticed that while relaxing the atomic configurations in a chain, atoms were allowed to move in the x- and y-directions until the minimum energy state was achieved. This resulted in a zig-zag geometry chain with optimum bond angles and bond lengths, which are displayed in figure 2.

The work reported earlier on atomic chains suggests that the zig-zag arrangement of infinite chains have a clear parallel in actual MCBJEs and the existence of a zig-zag minimum is a necessary condition for its appearance in finite-sized atomic chains in MCBJEs [17]. We have computed structural parameters, electronic band structure and dielectric function for four optimised bimetallic atomic chains of Au–Ag and Au–Pt, using the infinite chain model. On comparing the chain structures of types A and B, we find that the bond angles and bond lengths between the Au and Ag(Pt) atoms in type-A are different from that in type-B. This difference in bond angles and bond lengths can give rise to different kinds of electronic and magnetic properties of type-A compared to that of type-B.

Our computed cohesive energies for all relaxed structures of Au–Ag or Au–Pt are reported in table 1.

As can be seen from the table, the A-type Au–Ag and D-type Au–Pt chains have the lowest cohesive energy. It can therefore be inferred that the A-type Au–Ag and the D-type Au–Pt bimetallic chains are most likely to be formed during break junction experiments. The relative stability of different bimetallic atomic chains of Au–Ag has been studied earlier on the basis of enthalpy criteria and it has been found that (i) the increase in Ag concentration weakens the relative stability of the alloy chain and (ii) the average bond length of the alloy chains increases on enhancing Ag contents [18,19]. This has been attributed to the relativistic contraction of 6s orbital of Au atoms which makes the Au–Au and Au–Ag bond lengths smaller than the Ag–Ag bond lengths. In our studies too, the D-type of chains with higher Ag contents show the lowest cohesive energy and higher interatomic bond length. In another study based on thermodynamical considerations using the grand canonical framework, it has been concluded that the atomic chains with an alternating arrangement of Au and Ag atoms are the most stable among other compositions on stretching the Au–Ag nanowire [19]. Our results, which are based on the criteria of cohesive

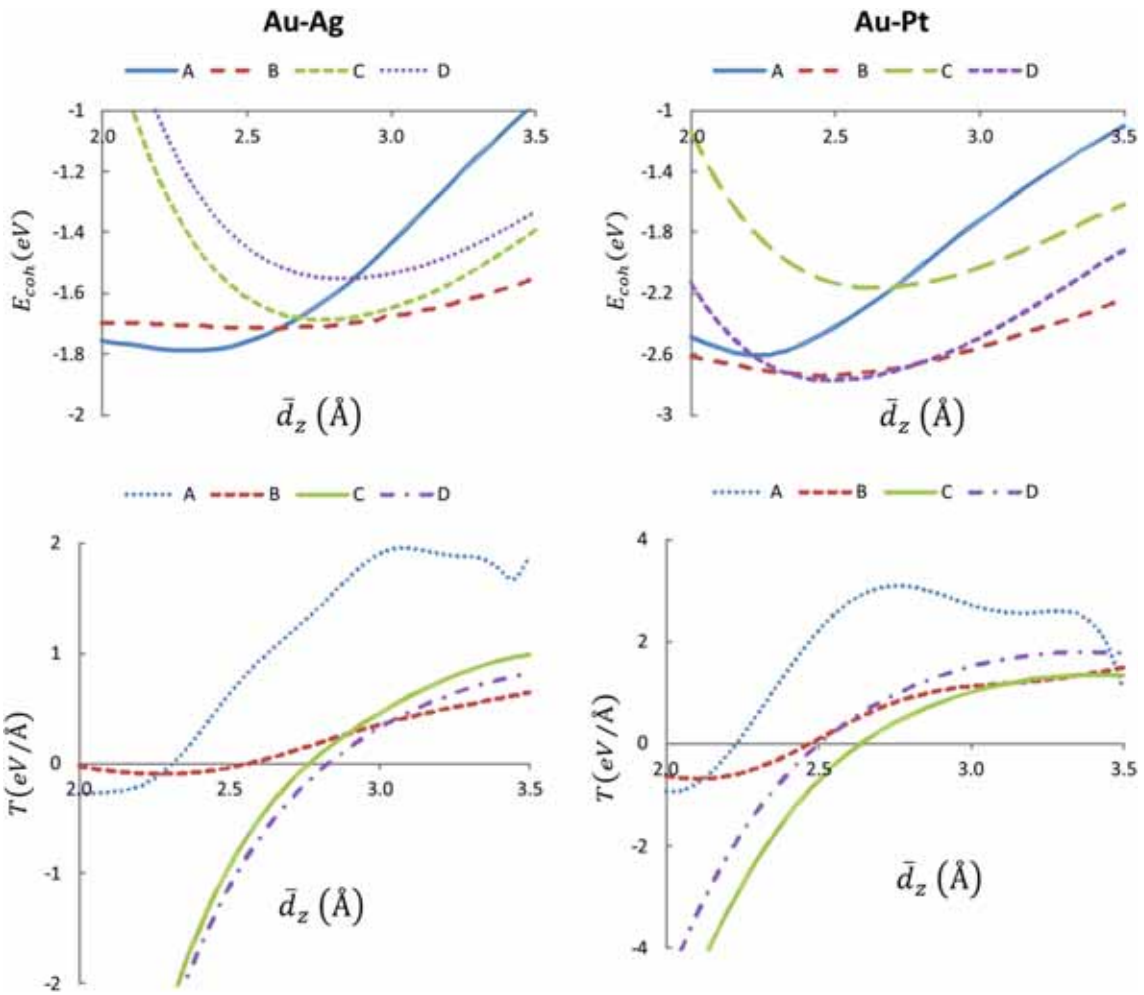

Figure 1. Variation of cohesive energy per atom E_{coh} and tension with average z-projected interatomic distance d_z for four types of Au–Ag and Au–Pt chain structures.

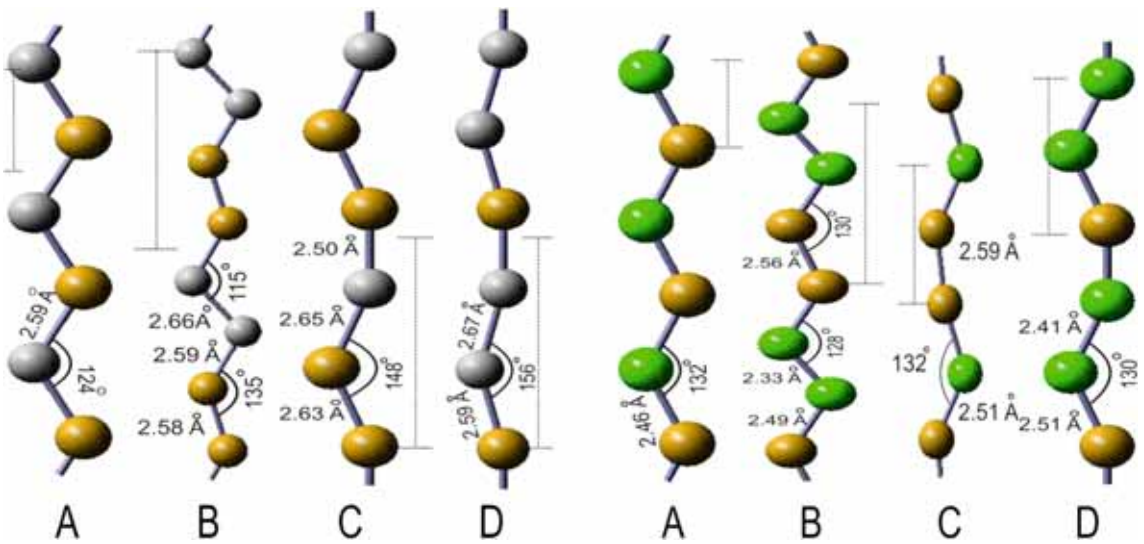

Figure 2. Four types of optimised chain structures of Au–Ag and Au–Pt exhibiting bond lengths and bond angles. Yellow and grey (green) spheres present the Au and Ag (Pt) atoms, respectively. Dotted lines show unit cells considered for the calculation.

Table 1. Cohesive energy and magnetic moment calculated for Au–Ag and Au–Pt atomic chains.

Composition type	E_{coh} (eV/atom)	Magnetic moment (μB)
Au–Ag A	−1.71	–
Au–Ag B	−1.66	–
Au–Ag C	−1.70	–
Au–Ag D	−1.46	–
Au–Pt A	−2.56	0.61
Au–Pt B	−2.66	0.76
Au–Pt C	−2.29	0.07
Au–Pt D	−2.82	1.15

energy and tension, also suggest that the A-type Au–Ag atomic chain, which has an alternating Ag and Au arrangement, is the most stable among other possible compositions. The trends of atomic chain formation for the Au–Pt atomic chains are completely different from those for Au–Ag. The most stable composition is the D-type that has more number of Pt atoms.

Calculations that include spin–orbit coupling show that all Au–Ag bimetallic atomic chains are non-magnetic, and the Au–Pt bimetallic atomic chains are magnetic if the number of Pt atoms is more than or equal to the number of Au atoms in a chain. The difference of total energies of non-magnetic (E_{NM}) and ferromagnetic (E_{FM}) states, $E_{NM}-E_{FM}$, for the Au–Pt chains of types A, B, C and D are found to be: 0.75, 1.43, 1.20 and 1.11 eV, respectively, suggesting that the ground states of all Au–Pt atomic chains are magnetic. As seen from table 1, the Au–Pt chain that has more Au atoms than Pt atoms gives rise to a negligibly small magnetism of 0.07 μB. Au atomic chains are found to be non-magnetic, while Pt chains with partially filled d-orbitals are magnetic. The chain of Ag atoms is non-magnetic [15]. Therefore, the Au–Pt chains exhibit magnetism, while the Au–Ag chains do not. It can therefore be said that the moment observed in the Au–Pt chains arises due to the hybridisation of the Au–Pt atomic orbital. As the magnetic moment along directions perpendicular to the z-axis is very small for all four structures, the major spin axis is the z-axis only. We therefore reported the magnetic moment only along the z-axis in table 1. Ultrathin Au–Pt nanowires have been found to be magnetic and the charge transfer mechanism is suggested as a source of observed ferromagnetism in the alloy nanowire of Au–Pt [27]. It has been reported that ferromagnetic moments stabilise the $Au_{48}Pt_{52}$ nanowires [27]. A similar trend is observed in our study too, where the D-type Au–Pt atomic chains shows the highest magnetic moment per atom and cohesive energy. This suggests that a relatively higher number of Pt atoms in a chain enhances the stability and the magnetic moment.

3.2 *Electronic and optical properties*

Both figure 1 and table 1 suggest that among the four chain structures of Au–Ag and Au–Pt, which are reported above, type-A Au–Ag and type-D Au–Pt chains are the most stable structures, as per cohesive energy and tension criteria for stable structures. We therefore can infer that type-A Au–Ag and type-D Au–Pt chains are most likely to be formed in a break junction experiment. In view of this, we computed the electronic band structure and the density of states for type-A Au–Ag and type-D Au–Pt atomic chains. Our results, with Fermi energy set to 0, are displayed in figure 3.

As seen from figure 3, type-A Au–Ag chain exhibits a band gap of 0.9 eV, and hence it can be termed as a semiconducting chain. In the case of type-D Au–Pt atomic chain, two bands are crossing the Fermi level and hence it can be considered as a metallic chain. The number of bands that crosses the Fermi level determines the ballistic quantum conductance of a wire, nG_0, where n is the number of bands that crosses the Fermi level. The ballistic conductance of $2G_0$ for pristine Au and Ag and $3G_0$ for Pt atomic chains with zig-zag geometry has been reported in [11]. Unlike the pristine Au and Ag zig-zag chains (which exhibit metallic behaviour) [11,15,22], bimetallic Au–Ag chains show semiconducting behaviour. The existence of a gap in our computed electronic structure Au–Ag type-A atomic chain indicates that the electronic properties change from metallic to semiconducting on alloying Au and Ag atoms in a chain. Type-A Au–Ag chain is an evenly alloyed chain that has an equal number of Au and Ag atoms in a supercell, while type-D Au–Pt chain is an unevenly alloyed chain with one Au and two Pt atoms per unit cell. Atomic arrangement in a unit cell makes type-A very different from types B, C and D. Ground-state band structure effects of type-A Au–Ag chain can therefore be different from other types of chains. Hence, type-A exhibits semiconducting behaviour, while types B, C and D Au–Ag chains display metallic behaviour. It has been suggested that the semiconducting nature of the bimetallic chain of Au–Ag may be due to the ground-state band structure effects [35].

As seen from figure 3, two bands cross the Fermi energy level for a type-D Au–Pt chain, which gives rise to $2G_0$ quantum conductance. One of the bands that crosses the Fermi level, in the case of the type-D Au–Pt chain, is more dispersive. This can be attributed to the hybridised S and d_z^2 orbitals of Au and Pt atoms. The presence of a larger dispersive band in the type-D Au–Pt chain is an indication of a stronger σ-bond that provides a greater stability to the Au–Pt chain structures.

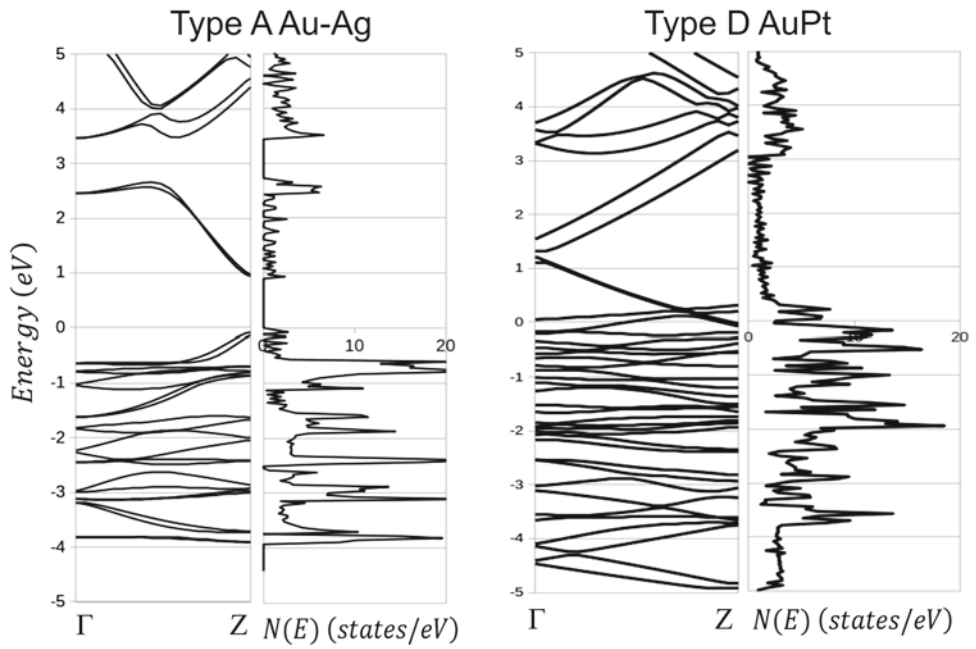

Figure 3. Electronic band structure and density of states for the type-A Au–Ag and the type-D Au–Pt atomic chains depicted in figure 2.

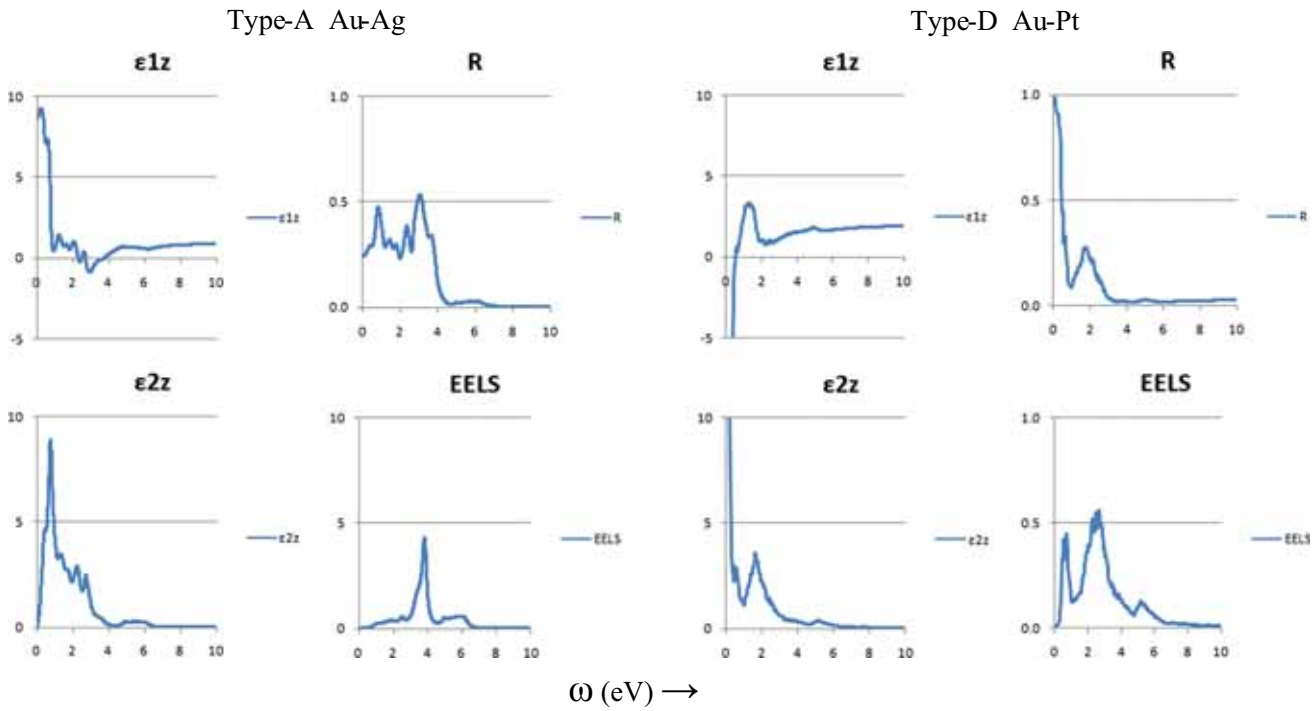

Figure 4. Real and imaginary parts of the dielectric function, reflectivity and electron energy loss spectrum for the type-A Au–Ag and the type-D Au–Pt atomic chains.

Optical parameters like reflectivity, absorption spectra and electron energy loss spectra can be obtained from the real (ε_1) and imaginary (ε_2) parts of the dielectric function. We computed ε_1 and ε_2, reflectivity and electron energy loss spectra, as a function of photon energy for the type-A Au–Ag and the type-D Au–Pt chains, which are the most stable chain structures as per our findings. Our computed results as a function of photon energy are plotted in figure 4.

For computing optical parameters, we incorporated both intraband and interband contributions for the type-D Au–Pt chain, while intraband contributions (Drude term) are not included for type-A Au–Ag chain. The peak in ε_2 for a semiconducting chain of Au–Ag corresponds to the transitions across a band gap of 0.9 eV. The band gap of 0.9 eV that falls within the infrared regime of the spectrum (0.01–1.7 eV) suggests that the A-type Au–Ag chain can be useful for making infrared devices. A sharp dip in the reflectance spectra and the peak in electron energy loss spectra, which correspond to collective excitations, are also seen for the type-A Au–Ag chain at around 3.9 eV. On comparing our computed optical parameters of the Au–Pt chain with that of the pristine chains of Au and Pt [22], we find that the behaviour of the optical parameters of the bimetallic Au–Pt chain is very similar to that of the zig-zag Pt chain. We further find that the electron energy loss spectra of the type-D Au–Pt chain exhibit two peaks at 0.71 and 2.25 eV, respectively. Plasma frequencies for the Au zig-zag chain have been reported at 1.11 eV, while the Pt zig-zag chain shows two peaks in EELS at 0.59 and 1.67 eV [22]. Thus, a shift towards a higher frequency is observed when the Pt-atomic chain is replaced with the bimetallic Au–Pt chain.

4. Conclusion

We have studied the structural parameters and the electronic and optical properties of the free-standing bimetallic linear atomic chains made of Au–Ag and Au–Pt, which have equal and unequal number of two different types of atoms. Based on the criteria of cohesive energy and the tension parameter, all structures are found to form a zig-zag chain. Furthermore, the A-type Au–Ag chain and the D-type Au–Pt chain exhibit the lowest energy among all possible chain structures we have studied. It can therefore be inferred that the A-type Au–Ag and the D-type Au–Pt chains are the most stable chains among other possible bimetallic atomic chains and these have maximum probability of formation in the MCBJ experiments. All compositions of the Au–Pt atomic chains are found to be magnetic, where the magnetic moment mainly depends on the number of Pt atoms in a chain and not on the arrangement of atoms. The electronic band structure and density of states suggest that the A-type Au–Ag chain is semiconducting with a band gap of 0.9 eV. The type-D Au–Pt chain is found to be metallic in nature.

Acknowledgement

Ms Mudra R Dave acknowledges the financial support received from the University Grants Commission, New Delhi in the form of a UGC-BSR fellowship.

References

[1] S Link, Z L Wang and M A El-Sayed, *Phys. Chem. B* **103**, 3529 (1999)
[2] F Sato *et al*, *Appl. Phys. A: Mater. Sci. Process*. **81**, 1527 (2005)
[3] J M Krans, J M van Ruitenbeek, V V Fisun, I K Yanson and L J Jongh, *Nature (London)* **375**, 767 (1995)
[4] C J Muller, J M Ruitenbeek and L J de Jongh, *Physica C* **191**, 485 (1992)
[5] H Ohnishi, Y Kondo and K Takayanagi, *Nature (London)* **395**, 780 (1998)
[6] V Rodrigues, T Führer and D Ugarte, *Phys. Rev. Lett*. **85**, 4124 (2000)
[7] V Rodgrigues and D Ugarte, *Phys. Rev. B* **63**, 073405 (2001)
[8] T Kizuka, S Umehaa and S Fujisawa, *Jpn. J. Appl. Phys*. **L71(Part 1)**, 240 (2001)
[9] H Koizumi, Y Oshima, Y Kondo and K Takayanagi, *Ultra Microsc*. **17**, 88 (2001)
[10] D Snchez-Portal, E Artacho, J Junquera, P Ordejn, A Garca and J M Soler, *Phys. Rev. Lett*. **83**, 3884 (1999)
[11] S R Bahn and K W Jacobsen, *Phys. Rev. Lett*. **87**, 266101 (2001)
[12] A Hasmy, L Rincón, R Hernández, V Mujica, M Márquez and C González, *Phys. Rev. B* **78**, 115409 (2008)
[13] E M Smelova, A L Klavsyuk, K M Tsysar and A M Saletskii, *Moscow Univ. Phys. Bull*. **68**, 92 (2013)
[14] E Z da Silva, F D Novaes, A J R da Silva and A Fazzio, *Phys. Rev. B* **69**, 115411 (2004)
[15] J C Tung and G Y Guo, *Phys. Rev. B* **81**, 094422 (2010)
[16] E Tosatti, S Prestipino, S Kostlmeier, A Dal Corso and F D Di Tolla, *Science* **12**, 291 (2001)
[17] L F Seivane, V M Garca-Surez and J Ferrer, *Phys. Rev. B* **75**, 075415 (2007)
[18] W Fa and J Dong, *J. Chem. Phys*. **128**, 244703 (2008)
[19] P A da Silva Autreto, D S Galvaoand and E Artacho, *J. Phys.: Condens. Matter* **26**, 435304 (2014)
[20] C Ataca, S Cahangirov, E Durgun, Y R Jang and S Ciraci, *Phys. Rev. B* **77**, 214413 (2008)
[21] A Delin and E Tosatti, *J. Phys.: Condens. Matter* **16**, 8061 (2004)
[22] A Kumar, A Kumar and P K Ahluwalia, *Physica E* **46**, 259 (2012)
[23] A I Yanson, G Rubio-Bollinger, H E van den Brom, N Agraït and J M van Ruitenbeek, *Nature (London)* **395**, 783 (1998)
[24] P Z Coura, S B Legoas, A S Moreira, F Sato, V Rodrigues, S O Dantas, D Ugarte and D S Galva, *Nano Lett*. **4**(**7**), 1187 (2004)

[25] A L Klavsyuka, S V Kolesnikov, I K Gainullin and A M Saletsky, *Eur. Phys. J. B* **5**, 331 (2012)
[26] J Bettini *et al*, *Nat. Nano Technol*. **1**, 182 (2006)
[27] X Teng *et al*, *Nano Lett*. **9**(**9**), 3177 (2009)
[28] A Md Asaduzzaman and M Springborg, *Phys. Rev. B* **72**, 165422 (2005)
[29] P E Blochl, *Phys. Rev. B* **50**, 17953 (1994); G Kresse and D Joubert, *Phys. Rev. B* **59**, 17958 (1999)
[30] G Kresse and J Hafner, *Phys. Rev. B* **48**, 13115 (1993)
[31] G Kresse and J Furthmller, *Comput. Mater. Sci*. **6**, 15 (1996)
[32] J P Perdew, K Burke and M Ernzerhof, *Phys. Rev. Lett*. **77**, 3865 (1996)
[33] H J Monkhorst and J D Pack, *Phys. Rev. B* **13**, 5188 (1976)
[34] G P Francis and M C Payne, *J. Phys.: Condens. Matter* **2**, 4395 (1990)
[35] R Peierls, *Surprises in theoretical physics* (Princeton University Press, Princeton, 1979)